Polymer Journal (2018) 50:389–396
https://doi.org/10.1038/s41428-018-0023-0

ORIGINAL ARTICLE

Inducing defects in ordered mesoporous carbons via the block copolymer-templated high-temperature carbonization of nitrogen-containing polymeric precursors

Ling Gao[1] · Alvin Chandra[1] · Yuta Nabae[1] · Teruaki Hayakawa[1,2]

Received: 16 November 2017 / Revised: 15 December 2017 / Accepted: 19 December 2017 / Published online: 5 March 2018

Abstract

Structural defects in graphene directly influence its electronic structure and can lead to the development of unique properties. However, the introduction of defects into ordered mesoporous graphitic carbons has yet to be demonstrated. Herein, defects were successfully introduced into the graphitic carbon lattice of well-ordered hexagonal mesoporous carbons via a block copolymer soft-template method and high-temperature carbonization. Small-angle X-ray scattering, scanning electron microscopy, and nitrogen adsorption measurements revealed that well-ordered ~4 nm cylindrical mesoporous structures with high surface areas (532 m^2g^{-1}) and good mesoporosity were maintained after high-temperature carbonization up to 1500 °C and mechanical milling. Raman and CHN elemental analyses suggested that defects were introduced into the graphitic carbon lattice through surface reconstruction induced by N-atom removal during heat treatment. The obtained robust and well-ordered N-containing mesoporous carbons with deliberately introduced defects are considered promising materials for electrochemical reactions and as catalyst supports.

Introduction

Carbon-based nanomaterials such as graphene [1–6] and mesoporous carbons (MCs) [7, 8] have received increasing attention from scientists and engineers in recent years. Particularly, the ability to control defect introduction into carbon-based nanomaterials needs to be developed because the structural defects in carbon lattices have an enormous influence on the mechanical properties, thermal conductivity, and electrical conductivity of such carbon-based nanomaterials [1–3, 7, 8]. Introducing defects into graphene and well-ordered structures such as MCs has been reported to improve their reactivity and reliability, enhancing their potential for applications in energy storage [9] and electrocatalysis [10, 11]. However, although structural defects in the carbon lattice strongly affect such electrocatalytic reactions, methods for inducing defects in ordered MCs are not yet well established [12, 13]. This can be attributed to the high-temperature carbonization required for defect introduction; a process that tends to cause the structural collapse of ordered mesopores. Nevertheless, due to the unique characteristics of well-ordered MCs [14–18] including a high surface area, a uniform pore structure, and tunable pore sizes, well-ordered defect-induced MCs will be quite attractive as novel functional materials. To introduce defects into well-ordered MCs, novel methods must be developed.

In this study, well-ordered and hexagonally packed MCs with structural defects in their carbon lattice were successfully obtained by applying high-temperature carbonization and block copolymer (BCP)-templating to nitrogen (N)-containing polymeric precursors. High-temperature heat treatment of N-containing carbon-based systems allows for the development of defects in the carbon lattice by simple

✉ Teruaki Hayakawa
hayakawa.t.ac@m.titech.ac.jp

[1] Department of Materials Science and Engineering, School of Materials and Chemical Technology, Tokyo Institute of Technology, 2-12-1-S8-36 O-okayama, Meguro-ku, Tokyo 152-0033, Japan

[2] Precursory Research for Embryonic Science and Technology (PRESTO), Japan Science and Technology Agency (JST), 4-1-8 Honcho, Kawaguchi, Saitama 332-0012, Japan

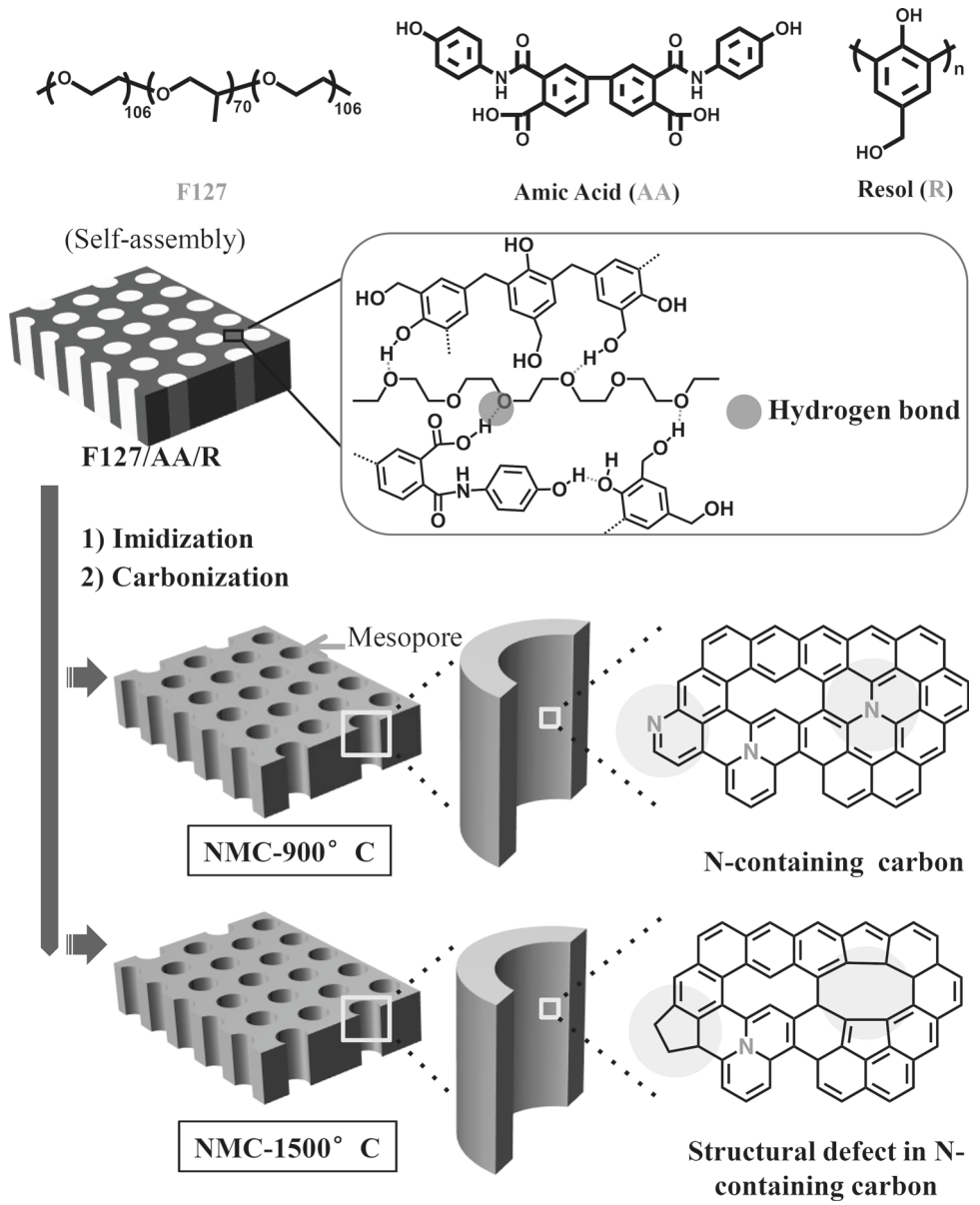

Scheme 1 Schematic illustration of the synthesis of defect-induced N-containing mesoporous carbons (purple matrix: PEO block/AA/R; yellow cylinders: PPO block) via the F127 BCP-assisted self-assembly of an aromatic N-containing carbon precursor, amic acid (AA), and a crosslinker, resol (R). Imidization and high-temperature carbonization under a N_2 atmosphere was used to obtain N-containing graphitic carbons with well-ordered mesopores (NMC-900 °C (gray, heated at 900 °C) and NMC-1500 °C (gray, heated at 1500 °C)) Structural defects could be introduced into the well-ordered mesoporous carbons by N-atom removal from the carbon lattice of NMC-1500 °C

pyrolysis [19–24]. As the N atoms are removed to yield multiple single-atom vacancies, defects in the carbon lattice (e.g., pentagons, heptagons, octagons) form via atom reconstruction. The use of N-containing aromatic amic acids (AAs) as the carbon precursor allows for the easy formation of graphene layers with a precisely controllable N-atom content for defect introduction in the carbon lattice. Additionally, the soft- [25–30] and hard- [12, 13, 31] template approaches are considered powerful tools for obtaining ordered and porous nanostructures. In contrast to the hard-template approach, the soft-template approach does not require post-synthesis template removal techniques that are typically carried out using harsh conditions, such as hydrogen fluoride etching. Furthermore, unlike the hard-template approach, which can be used to form structures based on only the minor domain of the template, the morphology of the carbon material can be adjusted easily (e.g., hexagonal cylinder minor or major domain) by tailoring the affinities and composition of the carbon precursors and the BCP template in the soft-template approach [32]. Shrinkage during the high-temperature carbonization process also increases the density and toughness of the matrix, allowing

for the direct synthesis of well-ordered MCs that can retain ordering even after defect introduction via high-temperature heat treatment.

In this article, we demonstrate the fabrication of well-ordered, defect-induced carbons with hexagonally packed mesoporous structures based on a N-containing system reported earlier (Scheme 1). Bulk films were prepared from a BCP template, Pluronic F127; an N-containing oligomeric precursor amic acid (AA); and a stabilizing cross-linker, resol (R). High-temperature pyrolysis was carried out at 900, 1100, 1300, and 1500 °C. Small-angle X-ray scattering (SAXS), scanning electron microscopy (SEM), Raman analysis, N_2 adsorption, and elemental analysis were then carried out to characterize the prepared defect-induced MCs.

Experimental procedure

Materials

The triblock copolymer Pluronic F127 ($M_w = 12\ 600$, PEO_{106}-PPO_{70}- PEO_{106}) was purchased from Sigma-Aldrich and used as received. Phenol, formalin (37% formaldehyde solution in methanol), 3,3,4,4-biphenyltetracarboxylic dianhydride (BPDA) and *p*-aminophenol (PAP) were purchased from the Tokyo Chemical Industry Co., Ltd. (TCI). BPDA and PAP were sublimated before use, while phenol and formalin were used as received. Sodium hydroxide (NaOH) was purchased from Wako Pure Chemical Industries, Ltd. The synthesis of the amic acid (AA) and resol (R) were described elsewhere [24, 33]. The obtained resol (R, $M_w = 535$, PDI = 1.30) was purified via column chromatography before use.

Synthesis of mesoporous defect-induced carbon

Polymer films (F127/AA/R) were prepared by mixing the Pluronic copolymer (F127), amic acid (AA) and resol (R) in a weight ratio of 50:12.4:37.6 wt% in DMF/EtOH (1:1 v), followed by solvent evaporation. After self-assembly had occurred, the obtained composite film was pyrolyzed under a nitrogen flow at 900 °C, 1100 °C, 1300 °C, and 1500 °C for 4 h. Then, mechanical grinding was conducted using a planetary ball mill (Fritsch, P7) and ZrO_2 beads (Nikkato, 0.5 mm) in an EtOH and H_2O solution to obtain well-ordered, mesoporous, defect-induced, N-containing mesoporous carbons (NMC-T, $T = 900$ °C, 1100 °C, 1300 °C, 1500 °C). The control samples (AA/R = 12.4:37.6 wt%) without the F127 template were prepared following the same heat treatment and milling processes. The obtained nitrogen-doped carbons were named NT-T ($T = 900$ °C, 1100 °C, 1300 °C, 1500 °C).

Characterization

Small-angle X-ray scattering (SAXS) data were obtained using a Bruker NanoSTAR (Bruker AXS K.K., Kanagawa, Japan, 50 kV per 100 mA) with a 2D-PSPC detector (camera length, 1055 nm). Nitrogen adsorption was performed using a Belsorp-mini II (Bel Japan Inc., Osaka, Japan), and these data were analyzed by the Barrett-Joyner-Halenda (BJH) method. Field emission scanning electron microscopy (FE-SEM; S-9000, Hitachi, Tokyo, Japan) was used with an accelerating voltage of 12.0 kV. Raman spectroscopy was performed using a JASCO RMP-510 spectrometer. X-ray diffraction (XRD) was performed using a Rigaku Ultima IV diffractometer with Cu Kα radiation. Elemental analysis was performed on a J-Science JM-10 analyzer.

Results and discussion

To investigate the properties of the well-ordered, defect-induced MCs, bulk films of both the well-ordered N-containing mesoporous carbons (NMCs) and the disordered nitrogen-containing carbons (NTs) were prepared. The NMC bulk films (F127/AA/R) were obtained from a blend of the Pluronic copolymer (F127), the nitrogen-containing precursor, amic acid (AA), and resol (R) stabilizer. After the selective self-assembly of AA and R with the PEO component in F127, well-ordered NMCs were obtained after pyrolysis. NT bulk films were prepared similarly but without the F127 BCP template. Additionally, since potential applications of NMCs typically require fine powders, mechanical milling was carried out after the thermal treatment processes, prior to further characterization.

Small-angle X-ray scattering (SAXS) was used to characterize the ordered structures of the as-prepared films after the heat treatment processes. The SAXS profile of the as-prepared film (Fig. 1) revealed scattering peaks with a $q{:}q^*$ ratio of 1:√3:√4 and a domain-spacing of 14.4 nm, suggesting that a hexagonally packed cylindrical structure had formed. Additionally, the ordered mesostructures were observed to have been retained after heat treatment at 900, 1100, 1300, and 1500 °C, where scattering peaks with $q{:}q^*$ ratios of 1:√3:√4:√7 and domain spacings of 9.7, 9.6, 9.5, and 9.5 nm, respectively, were observed. This indicates that the hexagonally arranged mesostructure was retained at high temperatures up to 1500 °C, even after having undergone the mechanical milling process. Additionally, the decrease in the domain spacing from 14.4 nm to 9.5 nm after pyrolysis above 900 °C indicates that the structure had become more compact and sturdy. In contrast, scattering peaks could not be observed in any of the NT bulk films prepared without the BCP template.

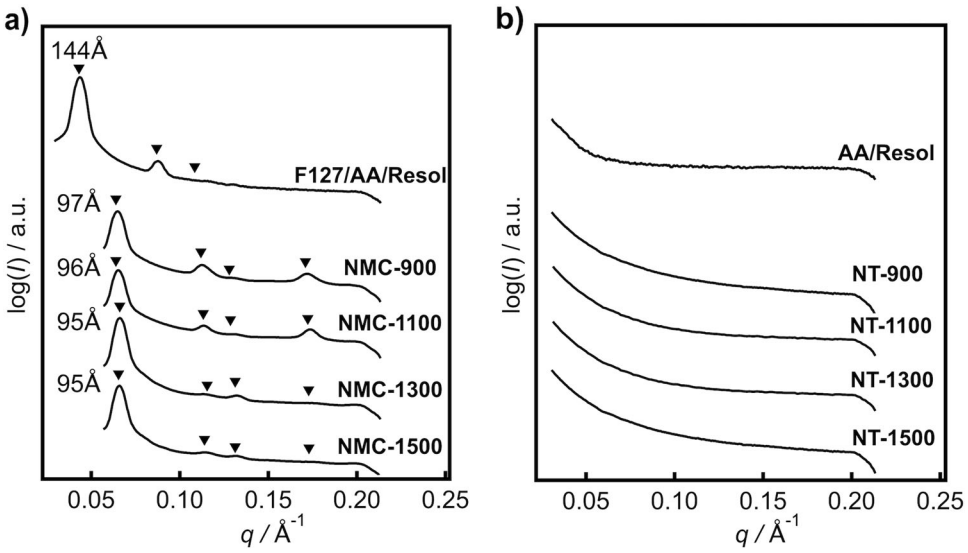

Fig. 1 The SAXS profiles of (**a**) the N-containing 2D-hexagonal mesoporous carbon (NMC) samples derived from the composite bulk films (F127/AA/R) and (**b**) the N-containing carbon samples derived from the control composite bulk films (NT) prepared without the F127 BCP template (AA/R), with carbonization at 900, 1100, 1300, and 1500 °C

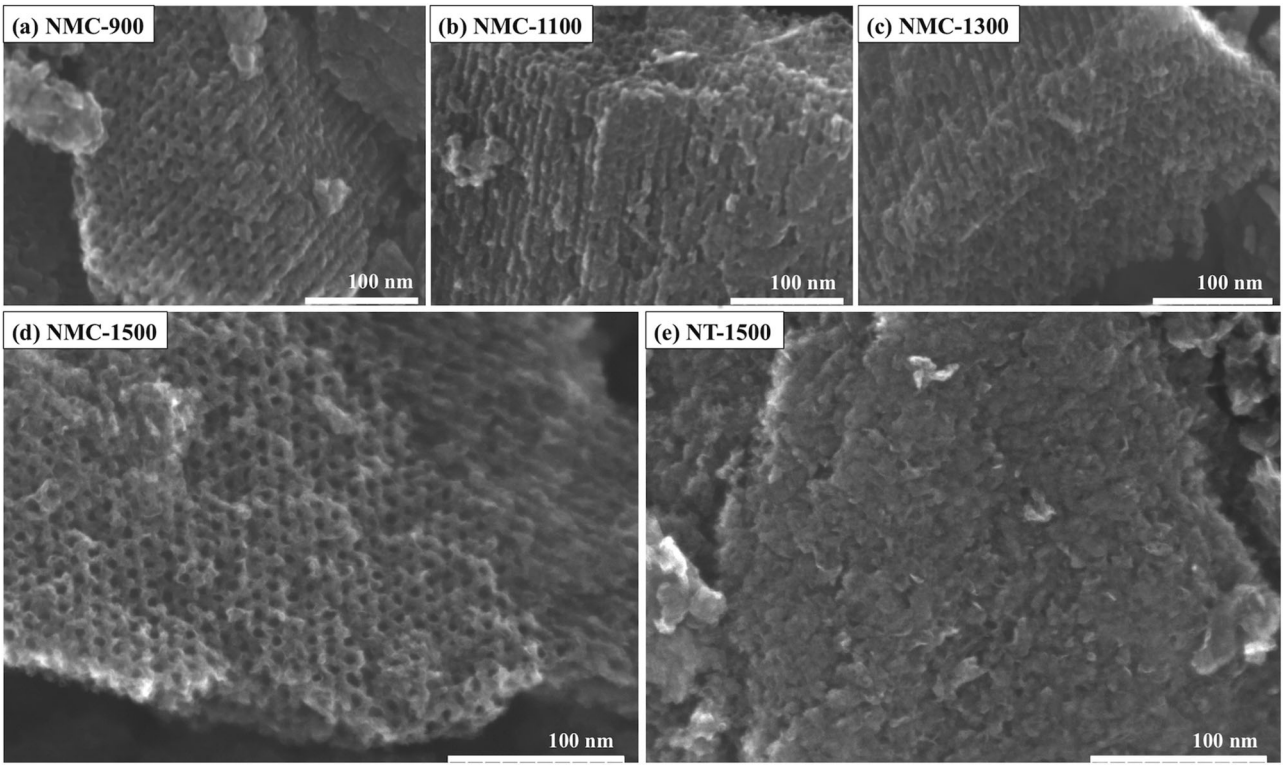

Fig. 2 FE-SEM images of (**a**) NMC-900, (**b**) NMC-1100, (**c**) NMC-1300, (**d**) NMC-1500, and (**e**) NT-1500

Further analyses of the bulk films were then conducted using field-emission scanning electron microscopy (FE-SEM) and X-ray diffraction (XRD) to directly observe and characterize the nanostructures formed. FE-SEM images of the thermally treated NMC-T and NT-T samples (T = pyrolysis temperature) were obtained (Fig. 2a-e). The FE-SEM images of NMC-T revealed the presence of uniform structures with hexagonally arranged cylindrical mesopores. Meanwhile, FE-SEM analysis of the NT-1500 sample revealed a disordered structure with poor porosity. Although the hard-template approach is limited to forming carbon structures in the mesoporous minor domain of the hard-template (e.g., individual cylindrical rods), the soft-template approach allows for the formation of interconnected mesoporous carbon structures based on the major domain of the BCP template. Furthermore, the FE-SEM

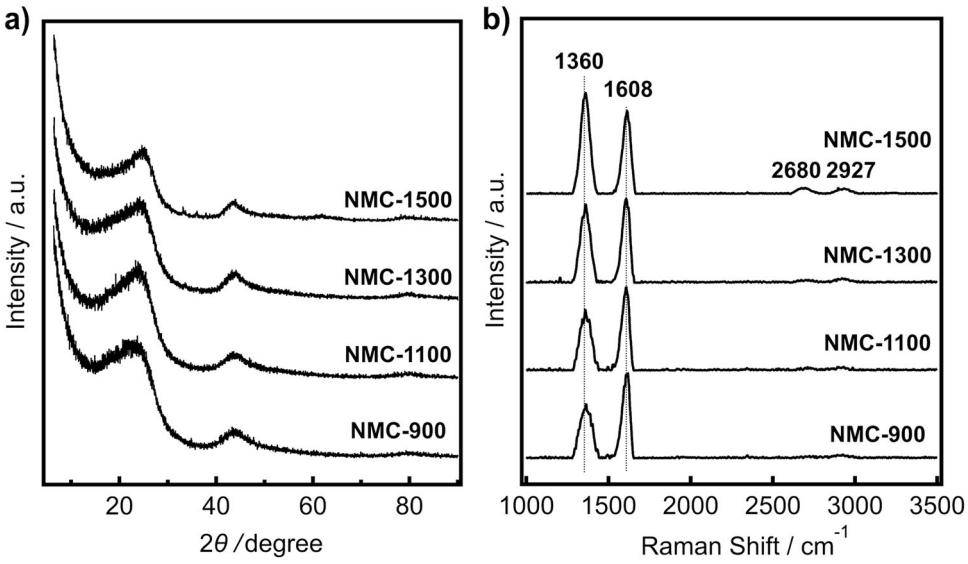

Fig. 3 (**a**) XRD profiles and (**b**) Raman spectra of N-containing ordered 2D-hexagonal mesoporous carbon (NMC) samples obtained from composite bulk films of F127/AA/R after carbonization

images revealed that well-ordered mesoporous structures could be retained after high temperature heat treatment at up to 1500 °C. The XRD profile (Fig. 3a) of the NMC-T samples revealed broad N peaks at ~23° and another relatively weak peak at approximately 43°. These diffraction peaks can be indexed to the (002) and (100) planes of the porous carbon walls, respectively. As the pyrolysis temperature was increased from 900 °C to 1500 °C, no obvious changes in the intensity or position of the peaks were observed. This suggests that near-maximum degrees of graphitization had been obtained.

To determine the degree of graphitization and defectivity of the carbon lattice after pyrolysis, Raman analysis was conducted (Fig. 3b). Peaks at 1360 cm^{-1} and 1608 cm^{-1}, corresponding to the D-band (disordered carbon) and G-band (graphitic carbon), respectively, could be clearly observed in the Raman spectra. For NMC-900, the intensity of the D-band is lower than that of the G-band, with an I_D/I_G ratio of 0.61, suggesting that a highly regular carbon structure with low defectivity had formed. As the temperature was increased from 1300 to 1500 °C, the ratio of I_D/I_G continually increased from 0.94 to 1.20, indicating that defects were introduced at higher pyrolysis temperatures. Moreover, two peaks with increasing intensity emerged, the 2D-band (2680 cm^{-1}) and G'-band (2927 cm^{-1}), which correspond to disorder-induced sp^2 graphitic carbon above 1300 °C. These results indicate that defects in the graphitic carbon lattice can be easily introduced above 1300 °C, potentially increasing the thermal and mechanical stabilities of the nanostructured NMCs.

To examine the mesoporosity of the NMC-T and NT-T carbon samples, N_2 adsorption analyses were conducted. The N_2 adsorption/desorption isotherms (Fig. 4) show that all the NMC-T samples exhibited type IV characteristics and a narrow pore size distribution, suggesting the presence of uniform mesopores. Meanwhile, the NT-T samples showed type II characteristics with no discernable pore size distribution. The Brunauer-Emmett-Teller (BET) specific surface areas were obtained based on the N_2 isotherms at 77 K, and the Barrett-Joyner-Halenda (BJH) method was utilized to calculate the mesopore volumes (V_{meso}). The BET specific surface areas (S_{BET}) of the well-ordered NMC-1500 (532 m^2g^{-1}) showed significant improvement over the S_{BET} of the analogous, disordered NT-1500 (386 m^2g^{-1}). Subsequently, BJH analysis indicated that narrow mesopores with diameters of approximately 4.2 to 4.8 nm had formed in the NMC-T samples. Although the total pore volumes (V_{total}) decreased with increasing heat treatment temperature, V_{meso} remained relatively constant at ~0.76 to 0.79 mL g^{-1} after heat treatment, a comparable value to those found in previous works [24, 33, 34]. This suggests that heat treatment selectively retained the mesopores, leading to a regular structure with a narrow mesopore size distribution.

As the chemical functionalities of NMCs depend heavily on the N content in the material, CHN elemental analysis was conducted to determine the concentration of N in the NMCs. Elemental analysis (Table 1) revealed that as the heat treatment temperature was increased, the carbon (C) content increased from 94.2 to 96.2 wt%, the hydrogen (H) content decreased from 0.46 to 0.06 wt%, and the N content decreased from 1.59 to 0.30 wt%. This suggests that as the temperature was increased, graphitization of the carbon framework occurred. Additionally, the decrease in the N content from 1.60 wt% upon heat treatment at 900 °C to 0.30 wt% at 1500 °C was likely due to the release of N atoms from the carbon lattice. Generally, there are four types of N precursors that can be used in the carbon lattice: pyridinic N, pyrrolic N, graphitic N, and oxidized pyridinic

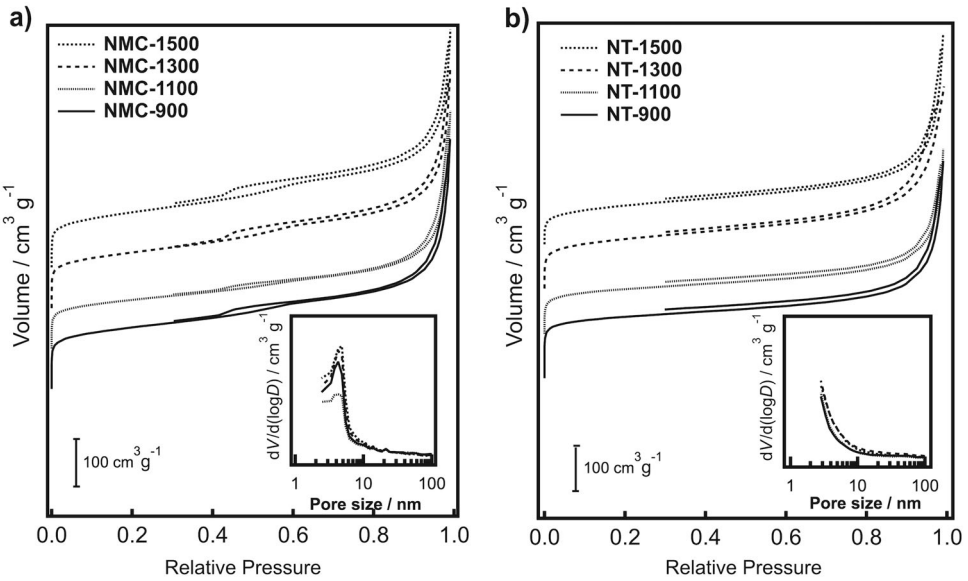

Fig. 4 **a** N_2 adsorption isotherms and pore size distributions of N-containing 2D-hexagonal mesoporous carbons and (**b**) of the control N-containing carbons prepared without the F127 BCP template. The isotherms were obtained at 77 K

Table 1 The mesoporosity data calculated from the N_2 adsorption and CHN elemental analysis results for the NMC samples with 2D-hexagonal structures and the control NT samples carbonized at varying temperatures

	d_{110}	S_{BET}	V_{total} [a]	V_{meso} [b]	D_{pore} [b]	Elemental analysis (wt%)		
Sample	(nm)	(m^2g^{-1})	(mLg^{-1})	(mLg^{-1})	(nm)	C	H	N
NMC-900	9.7	615	0.97	0.79	4.2	94.2	0.46	1.59
NMC-1100	9.6	494	0.91	0.76	4.2	94.6	0.17	1.07
NMC-1300	9.5	543	0.92	0.77	4.2	96.2	0.10	0.50
NMC-1500	9.5	532	0.90	0.76	4.8	96.2	0.06	0.30
NT-900	–	599	0.77	0.60	–	87.1	0.67	1.95
NT-1100	–	445	0.65	0.54	–	91.4	0.18	0.99
NT-1300	–	481	0.70	0.62	–	85.7	0.42	0.88
NT-1500	–	386	0.74	0.68	–	93.4	0.08	0.27

[a] Determined from the adsorption volume at $p/p^0 = 0.99$

[b] Calculated by the BJH method

N. At pyrolysis temperatures of ~800 °C, pyridinic N and pyrrolic N functionalities turn into graphitic N [11, 35, 36], whereas at temperatures much higher than 800 °C, N-atom removal from the carbon lattice can be expected. The removal of N atoms likely led to surface reconstructions and the formation of defects in the carbon lattice. Structural defects such as point defects and single- or multiple-atom vacancies typically appear on graphene layers during processing or growth. However, these defects are unstable and tend to migrate to reconstruct divacancies and form pentagons, heptagons, and octagons in the carbon lattice.

It is reasonable to hypothesize that the same defect formation mechanism exists in nitrogen-containing graphitic systems. Therefore, the removal of N atoms with increasing heat treatment temperatures allows us to introduce single- and multiple-atom vacancies, which are then likely reconstructed by migrating and combining configurations to form relatively stable defects (e.g., G(5775), G585) [2] in the carbon lattice. This defect formation mechanism due to N-atom removal is in good agreement with the results of the Raman analyses, where increasingly intense peaks corresponding to defects in the carbon lattice were observed with increasing heat treatment temperatures. Such well-ordered NMCs with low carbon contents (~0.3 wt%) and defects in the carbon lattice can be expected to exhibit effective catalytic activity for reactions such as hydrogen evolution (HER), oxygen reduction (ORR), and oxygen evolution (OER).

Conclusion

Well-ordered NMCs with hexagonally arranged, uniform, ~4 nm mesopores and defects in the carbon lattice were

successfully synthesized via the BCP soft-template approach. SAXS, SEM, and N_2 adsorption analyses revealed that well-ordered carbon structures with hexagonally arranged mesoporous cylinders (domain spacings = ~10 nm) and comparatively large mesopore volumes (V_{meso} = ~0.8 mL g^{-1}, V_{total} = ~0.9 mL g^{-1}) and specific surface areas (S_{BET} = 532 $m^2 g^{-1}$) were obtained after high-temperature carbonization and mechanical milling. The Raman spectra revealed that as the carbonization temperature was elevated from 900 to 1500 °C, the intensity of the 2D-peaks and G-peaks increased, suggesting that defects were successfully introduced into the graphitic carbon lattice. Meanwhile, CHN elemental analysis revealed that the nitrogen content decreased from approximately 2 to 0.3 wt % in both the NMC-T and NT-T samples after heat treatment at increasing temperatures. This could be attributed to the N-atom removal mechanism that occurs in NMCs heated above 1100 °C. It is likely that the removal of N atoms caused the formation of unstable single-vacancies and multiple-vacancies in the graphene layers that were then reconstructed to form C–C bonds and relatively stable carbon defects such as pentagons, heptagons, and octagons. By utilizing a method that combines BCP-assisted soft-templating and the high-temperature carbonization of N-containing polymeric precursors, NMCs with highly ordered mesopores (pore size of ~4.2 nm), a low pore size distribution, a high surface area (500–600 $m^2 g^{-1}$), and defect-inclusive graphitized carbons were developed. Using this novel approach, the formation of defect-induced MCs with controllable ordered structures based on BCP-assisted self-assembly (e.g., cylinder minor/major domain, double gyroid, etc.) can be carried out easily. Inducing defects in well-ordered MCs could further increase the potential for advanced functional applications.

Acknowledgements We are grateful to Ryohei Kikuchi of the Tokyo Institute of Technology, Ookayama, Materials Analysis Division, and Prof. Yuji Wada of the Tokyo Institute of Technology, Department of Chemical Science and Engineering, for assistance in the SEM measurements. We also would like to thank the Suzukakedai Materials Analysis Division, Technical Department, Tokyo Institute of Technology, for the CHN analysis. This work was partially funded by the Japan Science and Technology Agency (JST), the Precursory Research for Embryonic Science and Technology (PRESTO) on the Molecular Technology and Creation of New Functions.

Compliance with ethical standards

Conflict of interest The authors declare that they have no conflict of interest.

References

1. Banhart F, Kotakoski J, Krasheninnikov AV. Structural defects in graphene. ACS Nano. 2011;5:26–41.
2. Zhao H, Sun C, Jin Z, Wang D-W, Yan X, Chen Z, Zhu G, Yao X. Carbon for the oxygen reduction reaction: a defect mechanism. J Mater Chem A. 2015;3:11736–9.
3. Jia Y, Zhang L, Du A, Gao G, Chen J, Yan X, Brown CL, Yao X. Defect graphene as a trifunctional catalyst for electrochemical reactions. Adv Mater. 2016;28:9532–8.
4. Tao H, Gao Y, Talreja N, Guo F, Texter J, Yan C, Sun Z. Two-dimensional nanosheets for electrocatalysis in energy generation and conversion. J Mater Chem A. 2017;5:7257–84.
5. Cheng I, Hou Yi, Hu Y, Narita A, Müllen, K. Diels–Alder polymerization: a versatile synthetic method toward functional polyphenylenes, ladder polymers and graphene nanoribbons. Polym J. 2018;50:3-20.
6. Sun H-S, Chiu Y-C, Chen W-C. Renewable polymeric materials for electronic applications. Polym J. 2016;49:61–73.
7. Mohammadi N, Adeh NB, Najafi M. Synthesis and characterization of highly defective mesoporous carbon and its potential use in electrochemical sensors. RSC Adv. 2016;6:33419–25.
8. Goettmann F, Fischer A, Antonietti M, Thomas A. Chemical synthesis of mesoporous carbon nitrides using hard templates and their use as a metal-free catalyst for friedel–crafts reaction of benzene. Angew Chem Int Ed. 2006;45:4467–71.
9. Lin T, Chen I-W, Liu F, Yang C, Bi H, Xu F, Huang F. Nitrogen-doped mesoporous carbon of extraordinary capacitance for electrochemical energy storage. Science. 2015;350:1508–13.
10. Liu R, Wu D, Feng X, Müllen K. Nitrogen-doped ordered mesoporous graphitic arrays with high electrocatalytic activity for oxygen reduction. Angew Chem. 2010;122:2619–23.
11. Wan K, Long GF, Liu MY, Du L, Liang ZX, Tsiakaras P. Nitrogen-doped ordered mesoporous carbon: synthesis and active sites for electrocatalysis of oxygen reduction reaction. Appl Catal B Environ. 2015;165:566–71.
12. Wang H, Ding J, Zhang J, Wang C, Yang W, Ren H, Kong A. Fluorine and nitrogen co-doped ordered mesoporous carbon as a metal-free electrocatalyst for oxygen reduction reaction. RSC Adv. 2016;6:79928–33.
13. Wang X, He Z, Shi Y, Li B. Nitrogen-doped ordered mesoporous carbon as metal-free catalyst for power generation in single chamber microbial fuel cells. J Electrochem Soc. 2017;164:F620–7.
14. Wang J, Xin HL, Wang D. Recent progress on mesoporous carbon materials for advanced energy conversion and storage. Part Syst Charact. 2014;31:515–39.
15. Simon P, Gogotsi Y. Materials for electrochemical capacitors. Nat Mater. 2008;7:845–54.
16. Xin W, Song Y. Mesoporous carbons: recent advances in synthesis and typical applications. RSC Adv. 2015;5:83239–85.
17. Liang C, Li Z, Dai S. Mesoporous carbon materials: synthesis and modification. Angew Chem Int Ed. 2008;47:3696–717.
18. Fang Y, Lv Y, Che R, Wu H, Zhang X, Gu D, Zheng G, Zhao D. Two-dimensional mesoporous carbon nanosheets and their derived graphene nanosheets: synthesis and efficient lithium ion storage. J Am Chem Soc. 2013;135:1524–30.
19. Wang X, Liang C, Dai S. Facile synthesis of ordered mesoporous carbons with high thermal stability by self-assembly of resorcinol-formaldehyde and block copolymers under highly acidic conditions. Langmuir. 2008;24:7500–5.
20. Yu J, Guo M, Muhammad F, Wang A, Yu G, Ma H, Zhu G. Simple fabrication of an ordered nitrogen-doped mesoporous carbon with resorcinol-melamine-formaldehyde resin. Microporous Mesoporous Mater. 2014;190:117–27.
21. Cai T, Zhou M, Ren D, Han G, Guan S. Highly ordered mesoporous phenol-formaldehyde carbon as supercapacitor electrode material. J Power Sources. 2013;231:197–202.

22. Wei J, Zhou D, Sun Z, Deng Y, Xia Y, Zhao D. A controllable synthesis of rich nitrogen-doped ordered mesoporous carbon for CO2 capture and supercapacitors. Adv Funct Mater. 2013;23:2322–8.
23. Meng Y, Gu D, Zhang F, Shi Y, Cheng L, Feng D, Wu Z, Chen Z, Wan Y, Stein A, Zhao D. A family of highly ordered mesoporous polymer resin and carbon structures from organic-organic self-assembly. Chem Mater. 2006;18:4447–64.
24. Liu Y, Ohnishi K, Sugimoto S, Okuhara K, Maeda R, Nabae Y, Kakimoto M, Wang X, Hayakawa T. Well-ordered mesoporous polymers and carbons based on imide-incorporated soft materials. Polym Chem. 2014;5:6452–60.
25. Hsueh H-Y, Yao C-T, Ho R-M. Well-ordered nanohybrids and nanoporous materials from gyroid block copolymer templates. Chem Soc Rev. 2015;44:1974–2018.
26. Mun Y, Shim J, Kim K, Han JW, Kim S-K, Ye Y, Hwang J, Lee S, Jang J, Kim Y-T, Lee J. Direct access to aggregation-free and small intermetallic nanoparticles in ordered, large-pore mesoporous carbon for an electrocatalyst. RSC Adv. 2016;6:88255–64.
27. Tang J, Liu J, Li C, Li Y, Tade MO, Dai S, Yamauchi Y. Synthesis of nitrogen-doped mesoporous carbon spheres with extra-largepores through assembly of diblock copolymer micelles. Angew Chem Int Ed. 2015;54:588–93.
28. Jones BH, Lodge TP. Nanocasting nanoporous inorganic and organic materials from polymeric bicontinuous microemulsion templates. Polym J. 2012;44:131–46.
29. Wiesenauer BR, Gin DL. Nanoporous polymer materials based on self-organized, bicontinuous cubic lyotropic liquid crystal assemblies and their applications. Polym J. 2012;4415:461–8.
30. Sato K, Ishii K, Oaki Y, Nakanishi K, Imai H. Polymer-assisted shapeable synthesis of porous frameworks consisting of silica nanoparticles with mechanical property tuning. Polym J. 2017;49:825-30.
31. Sevilla M, Yu L, Fellinger TP, Fuertes AB, Titirici M-M. Polypyrrole-derived mesoporous nitrogen-doped carbons with intrinsic catalytic activity in the oxygen reduction reaction. RSC Adv. 2013;3:9904.
32. Wang K, Zhang J, Xia W, Zou R, Guo J, Gao Z, Yan W, Guo S, Xu Q. A dual templating route to three-dimensionally ordered mesoporous carbon nanonetworks: tuning the mesopore type for electrochemical performance optimization. J Mater Chem A. 2015;3:18867–73.
33. Nabae Y, Nagata S, Ohnishi K, Liu Y, Sheng L, Wang X, Hayakawa T. Block copolymer templated carbonization of nitrogen containing polymer to create fine and mesoporous carbon for oxygen reduction catalyst. J Polym Sci Part A Polym Chem. 2017;55:464–70.
34. Liang Y, Fu R, Wu D. Reactive template-induced self-assembly to ordered mesoporous polymeric and carbonaceous materials. ACS Nano. 2013;7:1748–54.
35. Sharifi T, Hu G, Jia X, Wågberg T. Formation of active sites for oxygen reduction reactions by transformation of nitrogen functionalities in nitrogen-doped carbon nanotubes. ACS Nano. 2012;6:8904–12.
36. Vinu A. Two-dimensional hexagonally-ordered mesoporous carbon nitrides with tunable pore diameter, surface area and nitrogen content. Adv Funct Mater. 2008;18:816–27.